

# Structural concrete behavior: coupled effect of drying and loading

L.Molez & Y.Berthaud

Laboratoire de Mécanique et Technologie, ENS Cachan / CNRS / Université Paris 6, France

D.Beaupré & B.Bissonnette

Centre de Recherche Interuniversitaire sur le Béton, Université Laval, Canada

**ABSTRACT:** Drying shrinkage may be a significant cause of deterioration of thin concrete repairs. Shrinkage-induced stresses can at least partially be relieved by tensile creep. Hydration effects and interface properties may have significant influence on concrete repair behaviour. An important experimental study was undertaken to understand the overall behaviour and to feed a numerical analysis tool. Different repair materials and setting techniques were studied. Long term and short term flexural tests were performed. Drying shrinkage and creep was found to be a very significant phenomenon for crack development. The used materials and setting techniques are shown to be very satisfying to restore structural capacity. The numerical formulation is presented in this paper. Both humidity effects and non-linear mechanical behaviour of the constitutive materials are taken into account. Phenomenological laws are used to describe mechanical damage and drying shrinkage. Moisture migration is described using a single diffusion equation. Numerical results show close agreement with experimental data.

## 1 INTRODUCTION

The field of concrete repairs has made considerable great strides for the few years and the tendency does not display any sign of deceleration. If search and knowledge are passably advanced in the field of new construction, however that of repair remains relatively misunderstood.

A very large amount of reinforced concrete structures world-wide are in a state of advanced deterioration. The defects are due to various causes, like errors in construction, accidental overloading, foundation failure, corrosion of reinforcement, fire attack or chemically hostile environment. Repairs should fulfil four basic requirements: arresting the deterioration of the structure, restoring the structural integrity, providing an aesthetically acceptable finish and, the last but not the least, being *durable* (Saucier 1990) (Emmons and Vaysburd 1994) (Bissonnette 1997). However, at the same time, it must also be conceded that many repaired structures are severely damaged after only a few years after being repaired (Vaysburd 2000). The cracking of the repair material causes the most serious deterioration processes leading to repair failures, since the aggressive agents can then penetrate through these cracks.

## 2 RESEARCH SIGNICANCE

The purpose of this investigation is to study the overall behaviour of repaired elements. We want to understand which are the significant parameters (hydration, shrinkage, creep, bond, etc.), and their relative importance, leading to the degradation of concrete repairs. We want to answer two questions. How to control the cracking of repairs? Is it possible to restore the structural integrity of repaired elements?

Facing to this problem, an important experimental study was undertaken. The generated data will feed a numerical analysis model that will permit to study various parameters and configurations.

## 3 THE CAUSE FOR CONCERN

A concrete repair can be defined as a thin concrete layer ( $\simeq 50$  to  $150$  mm) cast on an existing structure to replace the part close to the surface which is deteriorated. These two concrete layers have different mechanical and physical characteristics. The old one is quasi-stable with time. The new one change with time (hydration, drying shrinkage, creep). Some stresses are built-up as the sum of chemically, hygrally, thermally and mechanically induced strains increases (figure 1). The shrinkage and thermal

strains are restrained by the bond with the old layer. Tensile creep can partly relax these induced strains (Bissonnette 1997).

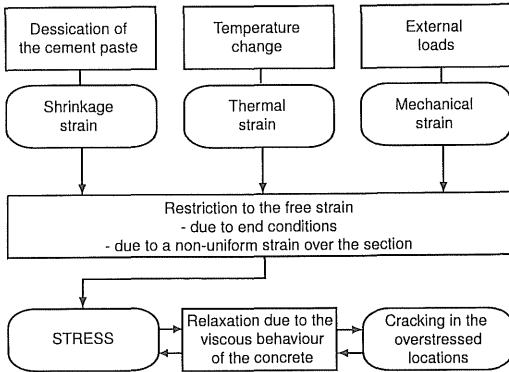


Figure 1: Schematic illustration of the stress build-up in repairs (Saucier et al. 1997).

## 4 EXPERIMENTAL WORK

### 4.1 Specimens

Previous studies carried out at Laval University (Pigeon et al. 1995) have shown that, with respect to crack development, it is important to perform the experiments on samples that are as close as possible to a real structure dimension-wise. The scale effects are very important and this is why the study has been done on large samples. All the selected materials (see section 4.3) were used to repair 4-meter long laboratory made reinforced concrete beams. The size and reinforcement details of the beams are given in figures 2 and 3. Thirty (five for each material)  $200\text{ mm} \times 300\text{ mm} \times 4000\text{ mm}$  beams were cast and moist-cured during 3 days. Ready mix concrete was used in the beams. The water to cement ratio was 0.40. The slump was  $100\text{ mm}$  and the air content was 5%. The average compression strength at 28 days was  $42\text{ MPa}$ . The shrinkage magnitude was about  $800\text{ }\mu\text{m}$  after 300 days. The beams were manufactured in august 1996 and exposed to outside conditions during 30 months and to laboratory conditions for 6 months before testing in order to simulate real aging.

### 4.2 Repair procedure

The same surface preparation technique was used before repairing all the beams. The bottom portion (tension strength zone) of the beam was chipped off, with a  $7.5\text{ kg}$  jack-drill, to a depth of  $75\text{ mm}$  on a length of 2 meters. Details can be seen in figure 3. The chipped surface was sandblasted to remove rust on reinforcement, carbonated concrete and loose particles. Before repairing, the surface was continuously humidified for 24 hours. Then, beams were repaired with the different materials (see section 4.3). The beams

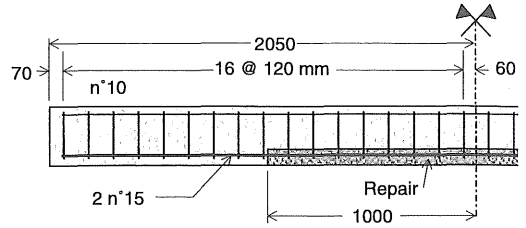


Figure 2: Test specimens.

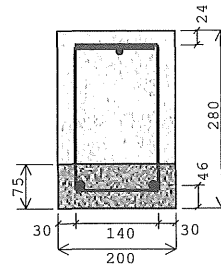


Figure 3: Section of test beams.

were wet-cured by covering them with wet burlap for 3 days and then allowed to dry during throughout the experiments.

### 4.3 Materials

Six different concretes were used to repair the damaged reinforced concrete beams. The choice of materials was carried out in order to obtain, on the one hand, similar mechanical properties and, on the other hand, a broad spectrum of amplitude of shrinkage and creep. Then, the water to cement ratio was fixed at 0.40. In order to obtain various values of shrinkage and creep, we adjusted the cement paste content of concretes (Neville 1996). The interface quality was "adjusted" by the setting technic. Previous study held at Laval University showed that ordinary cast-in-place concrete gives a poor quality interface, self-leveling concrete gives a good quality interface and shotcrete gives a very good quality interface (Lacombe et al. 1999). Composition of the repair materials can be seen in table 1. Two cast-in-place ordinary concrete were used (OC and SRA-OC). The second one has quite the same composition but with shrinkage reducing agent added. Two self-leveling concrete (SLC and LCC-SLC) were used. The first one can be considered as a "ordinary" self-leveling concrete. In the second one – low cement content self-leveling concrete – a part of cement was replaced by fly ash. The two last repair materials were shotcrete. The first one was a wet process shotcrete and the second one was a dry process shotcrete.

Table 1: Concrete mixture characteristics

	OC	SRA-OC	WSC *	SLC	LCC-SLC	DSC *
Cement T10 (kg)	400	400		412	235	400
Cement T10 SF (kg)			475			
Silica fume (kg)				37	20	40
Fly ash (kg)					214	
Water (kg)	162	158	190	180	188	176
Aggregate 10-2.5 (kg)	957	957	495	769	766	210
Sand (kg)	767	767	850	677	672	1450
Fiber (kg)			18			1
Air entraining agent (ml)	80	80	119	powder	powder	powder
SP(ml)	1800	1200	1675	powder	powder	
Colloidal agent				powder	powder	
Shrinkage reducing agent (ml)		8000				
Air (%)	8	8	14	12	8	6
E/L	0.40	0.40	0.40	0.40	0.40	0.40
S/(G+S)	0.440	0.44	0.630	0.459	0.458	0.869
Cement paste content (%)**	36/31	36/31	48/39.5	45/37	45/40	38/34

\* before projection

\*\* with the air content/without the air content

#### 4.4 Materials characteristics

The mechanical and hygrometric properties of the materials were characterized. Concrete cylinders of  $100\text{ mm} \times 200\text{ mm}$  were taken from ordinary and self-leveling concrete to measure compressive strength, splitting tensile strength and modulus of elasticity. For shotcrete, cores of  $75\text{ mm}$  diameter were taken from  $500\text{ mm} \times 500\text{ mm} \times 75\text{ mm}$  moulds. Drying shrinkage was monitored on  $100\text{ mm} \times 100\text{ mm} \times 350\text{ mm}$  prisms (cast or sawn). Tensile creep behaviour was obtained from  $75\text{ mm} \times 75\text{ mm} \times 400\text{ mm}$ . Tensile creep experimental procedure can be seen in (Bissonnette 1997).

Figure 4 give compressive strength versus time. It can be seen that we achieved to have six “similar” ma-

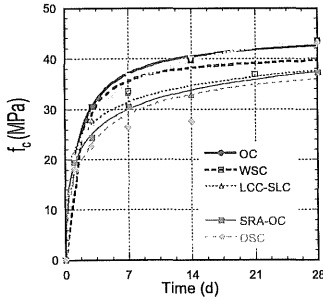


Figure 4: Compressive strength evolution.

terials in terms of strength. The tensile strength (figure 5) present a broader values variation. However, the tensile strength does not seem to have a significant influence (Bernard 2000). As we can see in figure 6, after 300 days, drying shrinkage measures are between  $400\text{ }\mu\text{m}/\text{m}$  and  $1050\text{ }\mu\text{m}/\text{m}$ . That makes it possible to study a significant drying shrinkage spectrum. Tensile creep was monitored during 3 months. Results can be seen in figure 7. Only four of the six materials has been tested until now. It can noticed that

two of the four materials present an important tensile creep. These two materials exhibit also a significant shrinkage. A comparison can be made by calculating the ratio between tensile creep and shrinkage (figure 8). This ratio can be used to evaluate the capacity of adaptation of materials. Tensile creep may relieve a part of restrained shrinkage (Bissonnette 1997). From this figure, it can be noted that the ratio becomes nearly constant after 2 weeks of testing. Values are between  $0.15$  and  $0.30\text{ MPa}^{-1}$ .

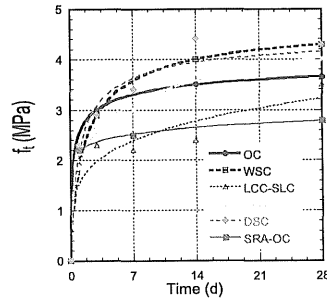


Figure 5: Tensile strength evolution.

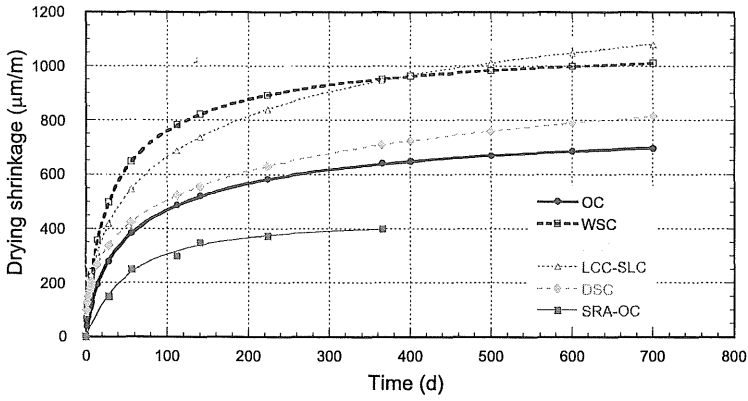


Figure 6: Drying shrinkage.

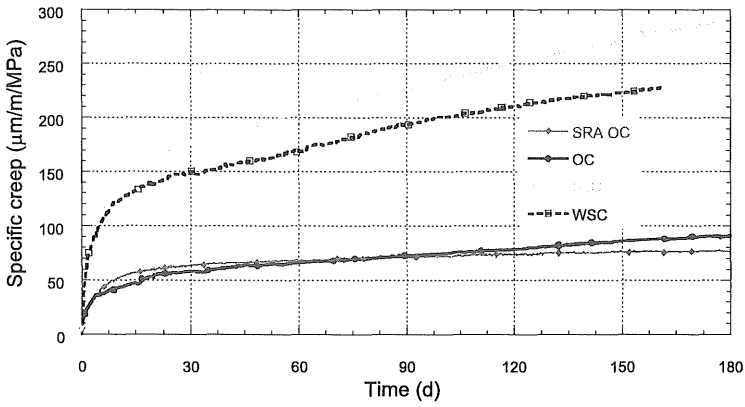


Figure 7: Specific tensile creep.

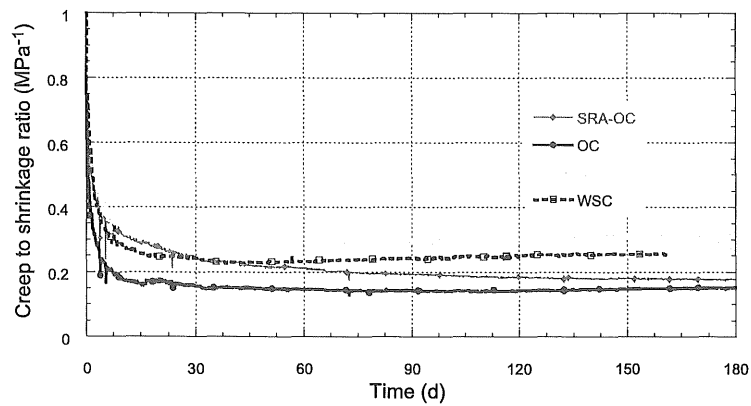


Figure 8: Specific creep to shrinkage ratio.

#### 4.5 Beams submitted to drying only

Repaired beams were monitored for 3 to 6 months in the laboratory. Two of the five beams repaired with each material were exposed to drying. After 3 days of curing, they were allowed to dry during throughout the experiments. For each beam, the crack propagation pattern was recorded. The surface cracks were monitored. A crack microscope with a magnification of 20X was used.  $5\ \mu\text{m}$ -cracks can be detected and cracks larger than  $25\ \mu\text{m}$  can easily be measured. The behavior of the repairs will be thus quantified by a series of crack parameters including the spacing, the opening and the length of cracks. Cracks were generally perpendicular to the principal axis of the beam. They usually appeared where stirrups were located. The crack opening was measured in five points across the beam width. The average crack opening is calculated by adding each width measurement for each crack on the average repair length and then dividing by the number of cracks.

Figure 9 gives the evolution of crack width for beams submitted to drying only. It has to be noted that beams repaired with ordinary concrete (OC) never crack even after 6 months of drying. The same behaviour is observed for ordinary concrete with shrinkage reducing agent (SRA-OC) after 28 days of drying. For all the other mix, first cracks appear after 5 or 7 days of drying. After 3 months of drying, the average crack width is between  $20\ \mu\text{m}$  for DSC and  $45\ \mu\text{m}$  for WSC. For WSC, after two months of drying, crack width seems to be stabilized. On the contrary, for SLC, LCC-SLC and DSC crack width continues to increase. The stabilization can be explained for WSC by the fibers content in this mix (see table 1). Fibers prevent large opening cracks by developing multi-cracked pattern. It can be noted that the mixtures that present the larger cracks are those who exhibit the more important drying shrinkage (see figure 6). SLC show the more important shrinkage values, but not the more important crack width. It can be explained by the high value of the creep to shrink-

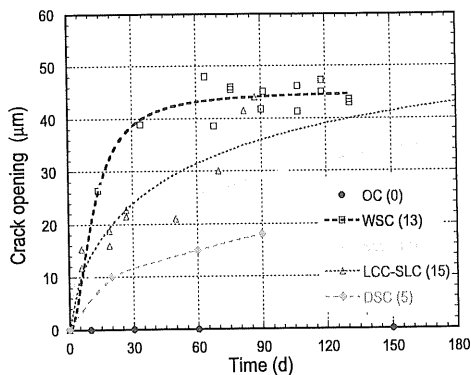


Figure 9: Crack width evolution - Drying only.

age ratio (see figure 8). The number of cracks after 6 months of drying is noted between () in figure 9.

#### 4.6 Beams submitted to drying and to long term loading

After 10 days of drying, two other beams, of each repair material, were subjected to drying and mechanical loading. They were tested as simply supported beams under four-point loading with a total loaded span of 3700 mm. They were loaded up to 33% of the theoretical ultimate load (equivalent to a service load in a high chemical aggressive environment). The last beam for each repair material, was loaded up to 66% of the calculated ultimate load (equivalent to a service load in a non-aggressive environment) after 45 days of drying.

##### 4.6.1 Test apparatus

The test apparatus can be seen in figure 10. Two beams were placed back to back and loaded under four-point loading as can be seen in figure 10. The load is applied at each end through springs. Those springs can partially compensate the effects of creep. With this type of equipment, a long-term load can be applied without monopolizing a closed loop testing system. It can be used in laboratory or outside in order to expose the repaired elements to severe environmental conditions. Each spring system was calibrated on a testing machine. Thus, the applied load could be known by measuring the deformation of springs. The load can be adjusted to 0.15 kN and is relatively constant in time. It had to be adjusted only twice during the 5 months of testing.

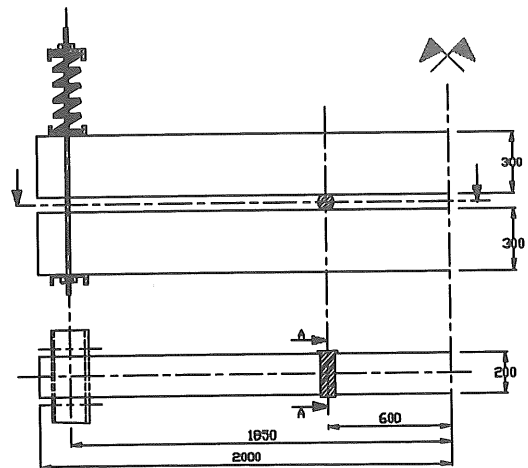


Figure 10: Loading setup

#### 4.6.2 Beams loaded to 33% of $P_{ult}$

Upon loading, the average crack opening was about  $50 \mu m$ , and after 4 months of drying, it increased to about  $85 \mu m$  for OC and DSC and  $100$  and  $125 \mu m$  for LCC-SLC and SLC respectively. It should be noted that almost no crack is lately created during the loading. The cracks previously created during the 10 days of drying open more at loading.

The crack width is quite similar for WSC and OC. On the other hand, WSC presents more cracks than OC. It can be explained by the larger shrinkage of WSC and the fibers content in WSC mix. SLC and LCC-SLC exhibit larger cracks than OC and WSC. This difference that appears just at loading, and up to a certain point, is due to mechanical properties mismatch. Finally, we could notice that during the four months of drying after loading, the crack width in-

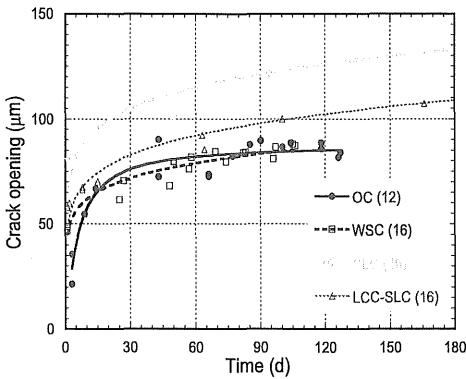


Figure 11: Crack width evolution - Loaded at 33%.

crease is quite similar for all mixtures and is equal to about  $50 \mu m$ .

#### 4.6.3 Beams loaded to 66% of $P_{ult}$

Upon loading, the average crack opening was about  $100 \mu m$  to  $125 \mu m$ . Firstly, we must note that WSC and SLC present the least open cracks. However, they display the greatest number of cracks. It can be explained by the fibers content, again, for WSC. The important creep to shrinkage ratio of SLC may explain these facts. Secondly, OC present again less cracks than other mixtures. Finally, the crack width increase is equal to  $25 \mu m$  for all mixtures. This last test was conducted 45 days after setting, and drying shrinkage kinetic is slower.

#### 4.7 Flexural testing

Previous tested beams (drying only series and 66% loaded series) were tested to rupture. The beams were loaded in four-point bending as previously with an hy-

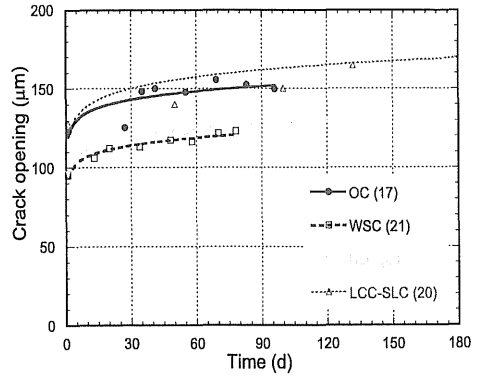


Figure 12: Crack width evolution - Loaded at 66%.

draulic testing machine. Deflection was recorded at midspan using two displacement transducers. The development and location of cracks was continuously observed until failure occurred.

The load-deflection curves for control beams and repaired beams is presented in figure 13. We extracted, from corresponding curves for the 8 repaired beams and 2 control beams, the load at first crack  $P_{cr}$ , the load at yield of reinforcement  $P_y$ , and the ultimate load  $P_u$ . Results are summarized in table 2. In this table  $P_u^{control}$  is defined by the average ultimate load for the two control beams. All repaired beams achieved the theoretical ultimate flexural capacity of  $65 \text{ kN}$ , presumably because failure was controlled by properties of parent concrete. Ductile flexural failures occurred, no interfacial bond breakdown was observed. The larger decrease (about 5 to 7%) of ultimate load was observed for OC beams.

These tests confirm that it is possible to restore the flexural behaviour of damage beams. No interfacial bond breakdown was observed as opposed to what literature usually says (Emberson and Mays 1996).

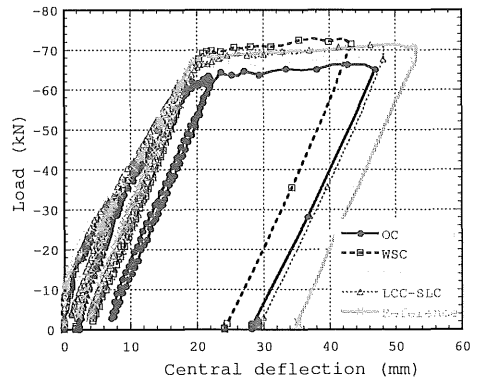


Figure 13: Flexural testing (drying only series).

## 5 TOWARDS A NUMERICAL ANALYSIS TOOL

Experimental results presented previously are often difficult to interpret. It is difficult to make distinction between the different effects of each parameter. A numerical analysis tools may help to understand the real behaviour of repaired beams and define global parameters to respect for good design of repaired elements.

We try to write a model that take into account the different physical phenomena. Phenomenological models are used to not complicate the numerical tool.

Table 2: Load deflection characteristics from short-term static tests

Repaired beams	$P_{cr}$ (kN)	$P_y$	$P_u$	$P_u/P_u^{control}$
Control 1	24	67.6	70.4	0.99
Control 2	-	68	71.6	1.01
OC-0	18	62	67.2	0.95
OC-66	-	62	66	0.93
WSC-0	20.4	68.8	72.8	1.02
WSC-66	-	68.8	72	1.01
SLC-0	21.6	65.8	70	0.99
SLC-66	-	68	72	1.01
LCC-SLC-0	24	65.6	71.6	1.01
LCC-SLC-66	-	64	67.6	0.95

### 5.1 Mechanical damage

In the present analysis, we use an isotropic scalar damage model (Mazars 1984). In this model, the mechanical effect of progressive micro-cracking due to external loads is described by a single internal variable which degrades the Young's modulus of the material. The constitutive relations are:

$$\sigma_{ij} = (1 - d)\Lambda_{ijkl}\varepsilon_{kl} \quad (1)$$

where  $\sigma_{ij}$  and  $\varepsilon_{kl}$  are the components of the stress and strain tensors respectively ( $i, j, k, l \in [1, 3]$ ), are the initial stiffness moduli, and  $d$  is the damage variable. The material is initially isotropic, with  $E$  and  $\nu$  the initial Young's modulus and Poisson's ratio respectively. Damage is a function of the positive strains which means that it is mainly due to micro cracks opening in tension mode. In order to avoid ill-posedness due to strain softening, the mechanical model has to be enriched with an internal length (Pijaudier-Cabot and Bažant 1987).

### 5.2 Non linear water diffusion equation

Moisture movements in concrete are of two types: a water flux in liquid form and a water flux in vapor form. The water consumption due to hydration is neglected. It is useful to write these movements as a function of the relative humidity  $H$  (Bažant and Najjar 1972). The relationship between  $H$  and  $w$  (the water content) at constant temperature  $T$  and at a fixed degree of hydration is given by the desorption or adsorption isotherms. The slope of isotherm is almost constant over the range of humidities  $0.15 \leq H \leq 0.95$  (Alvaredo 1994). Then moisture

movement can be written by a phenomenological diffusion equation:

$$\frac{\partial H}{\partial t} = D(H) \cdot grad H \quad (2)$$

The diffusion coefficient depend on  $H$ . When  $H$  is important, a reduction of the relative humidity causes a strong reduction of  $D$ . When  $H \leq 0.70$  to  $0.80$   $D(H)$  is almost constant. We choose the following expression of  $D(H)$  (Bažant and Najjar 1972):

$$D(H) = D_0 \left( \alpha_0 + \frac{1 - \alpha_0}{1 + \left(\frac{1-H}{1-H_c}\right)^n} \right) \quad (3)$$

where  $\alpha_0$ ,  $n$ , and  $H_c$  are adjustable parameters specific to material. This parameters can be determined from the "weight loss - time" relation.

Boundary conditions of the convective type are imposed at the surface  $\Gamma$  in contact with air at the relative humidity  $H_a$ :

$$q = \beta(H_\Gamma - H_a) \quad (4)$$

where  $q$  is the moisture flux normal to the exposed surface,  $\beta$  is the coefficient of surface hygral transfer and  $H_\Gamma$  is the relative humidity at the surface.

### 5.3 Shrinkage

Drying shrinkage can be explain by three theoretical mechanism: capillary depression, Gibbs-Bangham theory (surface tension) and disjoining pressure theory. A study was undertaken to take into account all these phenomena (Lassabatere 1994). This study shows that drying shrinkage can be well evaluated by a simple proportional equation:

$$\Delta\varepsilon_{sh} = \alpha_{sh}\Delta H \quad (5)$$

where  $\Delta H$  is the variation of relative humidity at the studied point and  $\alpha_{sh}$  is the of hydrous dilatation coefficient, by analogy with the thermal dilatation coefficient.

### 5.4 First results

Nonlinear finite element simulations of repaired beams was carried out. We used CASTEM 2000, the CEA finite element code. First results shown a good accuracy for prediction of humidity profile and

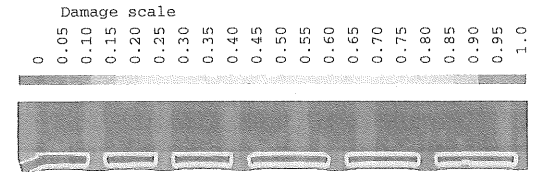


Figure 14: Damage due to restrained shrinkage in repaired beam

shrinkage. The crack pattern seemed to be in good agreement with experimental observations. A calculated crack pattern can be seen in figure 14.

## 6 CONCLUSIONS

- An important experimental study on real structure was undertaken. This study permitted the creation of a bank of data on concrete repairs.
- The effects of drying shrinkage do not to be neglected by repairs designers.
- Tensile creep can be a positive parameter. Tensile creep can partly relax induced strains. Creep to shrinkage ratio seems to be a good indicator for the choice of repair materials.
- Short term flexural test showed that it possible to restore flexural capacity of damage beams. Ductile flexural failures occurred in all studied repaired elements. No interfacial bond breakdown was observed.
- A numerical tool was proposed. This approach was based on phenomenological models including damage model, non linear diffusion theory and a shrinkage model. The finite element results were shown to be in good agreement with shrinkage behaviour and crack pattern.
- Much work remains to be done. On the experimental side, interfacial data have to be extracted. On the analytical side the finite element will benefit from an extension to account for creep, partially debonded interfaces and hydration effects.

## REFERENCES

- Alvaredo, A. M. (1994). *Drying shrinkage and crack formation*. Ph. D. thesis, Swiss federal institute of technology, Zurich, Swiss confederation.
- Bažant, Z. P. and L. J. Najjar (1972). Non-linear water diffusion in non-saturated concrete. *Materials and structures* 5(25).
- Bernard, O. (2000). *Comportement long terme d'éléments de structures formés de bétons d'âges différents*. Ph. D. thesis, Ecole Polytechnique Fédérale de Lausanne, Lausanne, Swiss confederation.
- Bissonnette, B. (1997). *Le fluage en traction: un aspect important de la problématique des réparations minces en béton*. Ph. D. thesis, Université Laval, Québec, Canada.
- Embersson, N. K. and G. C. Mays (1996). Significance of property mismatch in the patch repair of structural concrete. part 1,2,3. *Magazine of concrete research* 48(174).
- Emmons, P. H. and A. M. Vaysburd (1994). Factor affecting the durability of concrete repair: the contractor's viewpoint. *Construction and building materials* 8(1).
- Lacombe, P., D. Beaupré, and N. Pouliot (1999). Rheology and bonding characteristics of self-leveling concrete as a repair concrete. *Materials and structures* 32(222).
- Lassabatere, T. (1994). *Couplage hydromécanique en milieu poreux non saturé avec changement de phase : application au retrait de dessiccation*. Ph. D. thesis, Ecole nationale des ponts et chaussée, Paris, France.
- Mazars, J. (1984). *Application de la mécanique de l'endommagement au comportement non linéaire et à la rupture de béton de structure*. Ph. D. thesis, Université Paris VI.
- Neville, A. M. (1996). *Properties of concrete* (4th ed.). John Wiley & Sons, Inc.
- Pigeon, M., D. St. Pierre, M.-A. Bérubé, A. Lamontagne, and T. Sedran (1995). Steel fiber reinforced shotcrete repair of concrete structures affected by alkali-silica reaction: laboratory assesment. In *International conference on concrete under severe conditions: Environment and loading*, Sapporo, Japan.
- Pijaudier-Cabot, G. and Z. Bažant (1987). Nonlocal damage theory. *J. of Engrg. Mech.* 113.
- Saucier, F. (1990). *La durabilité de l'adhérence des réparations en béton*. Ph. D. thesis, Université Laval, Québec, Canada.
- Saucier, F., F. Claireaux, D. Cusson, and M. Pigeon (1997). The challenge of numerical modeling of strains and stresses in concrete repairs. *Cement and concrete research* 27(8).
- Vaysburd, A. M. (2000, August). Concrete problems, repair solutions and confusions - an attempt to establish the facts. In *Advances in cement and concrete: Materials aspects of concrete repairs and rehabilitation*, Mont-Tremblant, Quebec, Canada. United Engineering Foundation, Inc.